NANO LETTERS
Cite This: Nano Lett. XXXX, XXX, XXX−XXX
Letter
pubs.acs.org/NanoLett

Giant, Voltage Tuned, Quality Factors of Single Wall Carbon Nanotubes and Graphene at Room Temperature

A. Descombin, P. Poncharal, A. Pascale-Hamri, M. Choueib, R. Diehl, P. Vincent, S. T. Purcell, A. Ayari, and S. Perisanu*

Univ Lyon, Université Claude Bernard Lyon 1, CNRS, Institut Lumière Matière, F-69622, Villeurbanne, France

Supporting Information

ABSTRACT: Mastering dissipation in graphene-based nanostructures is still the major challenge in most fundamental and technological exploitations of these ultimate mechanical nanoresonators. Although high quality factors have been measured for carbon nanotubes (>10^6) and graphene (>10^5) at cryogenic temperatures, room-temperature values are orders of magnitude lower (≃10^2). We present here a controlled quality factor increase of up to ×10^3 for these basic carbon nanostructures when externally stressed like a guitar string. Quantitative agreement is found with theory attributing this decrease in dissipation to the decrease in viscoelastic losses inside the material, an effect enhanced by tunable "soft clamping". Quality factors exceeding 25 000 for SWCNTs and 5000 for graphene were obtained on several samples, reaching the limits of the graphene material itself. The combination of ultralow size and mass with high quality factors opens new perspectives for atomically localized force sensing and quantum computing as the coherence time exceeds state-of-the-art cryogenic devices.

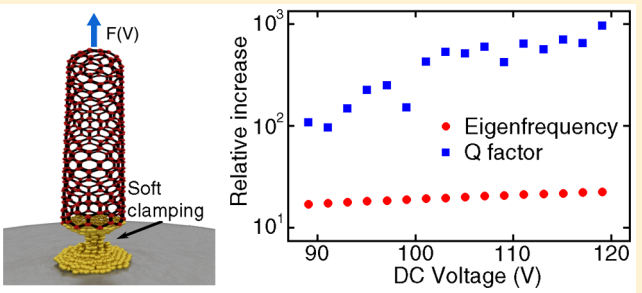

KEYWORDS: *NEMS, carbon nanotube, graphene, Q-factor, nanomechanics*

Decreasing dissipation is a ubiquitous topic of research in most fields of applied and fundamental physics, ranging from mechanical clocks to radio frequency devices,[1] fluctuations in gravitational waves detectors,[2] and to fluid flow mechanics. For resonators, it is quantified by the quality (Q) factor, given by the ratio of the stored energy E_S to the losses during one cycle E_D or, equivalently, the ratio of the eigenfrequency f to the frequency width Δf:

$$Q = 2\pi\frac{E_S}{E_D} = \frac{f}{\Delta f} \quad (1)$$

High Q-factors allow on the one hand less power consumption to maintain oscillation and on the other hand less fluctuations and better frequency resolution which is of critical importance for sensing as well as for quantum regime phenomena. Mechanical Q-factors have been shown to decrease with the volume of the resonator.[1,3] Because the stored energy is proportional to volume, this scaling means that dissipation is more of a surface effect.

For nanoscale sizes, there is now a better understanding of resonance broadening due to stochastic frequency shifts or dissipation through coupling with external channels such as adsorbates[4] and charge displacement.[5−8] However, for graphene-based nanostructures there is little comprehension of the intrinsic mechanisms leading to dissipation of the stored energy in the volume and/or at the clamping, mechanisms that set ultimate limits of the achievable Q-factors. On one hand, experimental values for graphene and single wall carbon nanotubes (SWCNT) Q-factors vary from $10^4 - 5 \times 10^6$ at cryogenic temperatures[9−15] to 50−150 at room temperature[14−18] with a highest value of 2300 for a graphene resonator.[3] On the other hand, theoretical simulations for the Q-factor of SWCNT with ideal clamping set high limits on the order of 10^5 at cryogenic temperatures and 10^3 at room temperature due to phononic mode coupling.[19] We have therefore experimental values that exceed theoretical limits for cryogenic temperatures by more than ×100 and diminish several orders of magnitude for room-temperature measurements, remaining a factor of 10 below theoretical predictions. Moreover, multiwall carbon nanotubes (MWCNT) are predicted to have lower Q-factors than SWCNTs due to friction between the walls, but we found room-temperature Q-factors of ≃10^3 in the literature for MWCNTs under high stress.[20] These room-temperature low Q-factors severely limit potential applications for graphene-based resonators. Going beyond the state of the art in mechanical dissipation of graphene requires understanding and characterizing effects inside the material as well as on the contact surface of the clamping in order to reduce both phonon coupling and external channels leading to energy losses.

We study here the Q-factor of individual SWCNTs and graphene sheets singly clamped at the apex of tungsten (W)

Received: October 24, 2018
Revised: January 18, 2019
Published: February 1, 2019

DOI: 10.1021/acs.nanolett.8b04282
Nano Lett. XXXX, XXX, XXX−XXX

tips in an ultrahigh vacuum (UHV) field emission (FE) environment at room temperature as presented on Figure 1a,b.

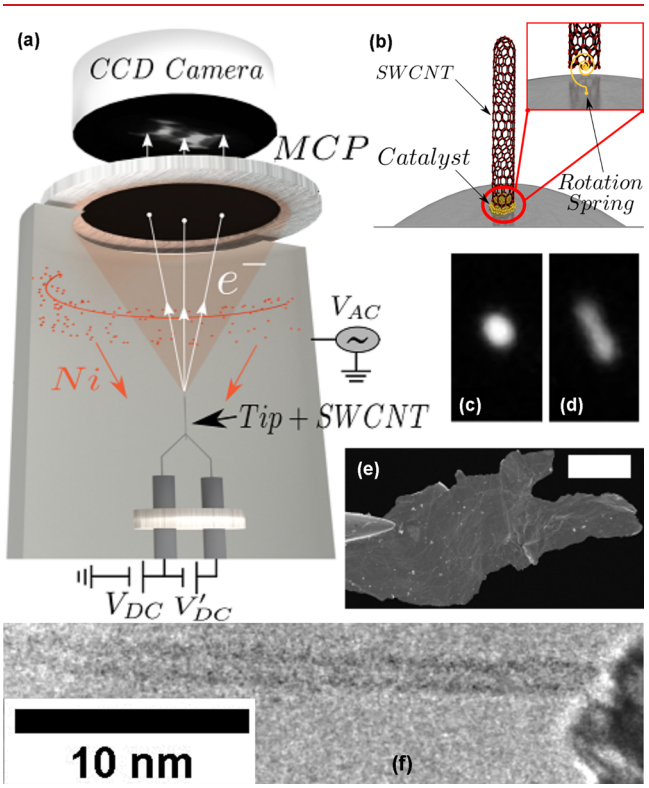

Figure 1. (a) Experimental UHV chamber with temperature controlled W tip and Ni catalyst deposition loop for in situ growth of SWCNT. (b) Zoom of the W tip apex with a SWCNT on a Ni nanoparticle. The inset represents the Ni nanoparticle acting as a rotation spring. (c,d) Electron field emission pattern from SWCNT4 out of resonance (c) and in resonance (d). (e) Scanning electron microscope image of the graphene monolayer sample G1 on a W tip. The white scale bar is 5 μm long. (f) Transmission electron microscope image of a typical in situ grown SWCNT giving a diameter of ≃1.1 nm.

The W tips were previously submitted to a carburization procedure optimized for low-resistance contacts in order to avoid Coulomb blockade phenomena[21] that can influence the measured Q-factor.[22,23] A high voltage V_{DC} is applied thus creating a strong, tip-enhanced, electric field at the nanostructure's apex and therefore inducing an important mechanical axial stress in the resonator. An electronic current is extracted from the nanostructure by the electric field[24−26] and it creates a FE pattern on a phosphor screen (Figure 1c,d) after amplification by a microchannel plate situated at 2−3 cm from the sample. Temperature-controlled in situ heating of the tip for cleaning or for SWCNT growth purposes[35] can be performed using the floating V'_{DC} source and the calibrated electric heating loop that supports the tip, as shown on Figure 1a. The V'_{DC} source is disconnected during the mechanical experiments, leaving the sample only in contact with the V_{DC} source. This field emission setup allows the study of nanostructures with highly reduced influence from the environment, minimizing additional dissipation channels as the samples are in contact with only the support tip on a very small surface (see Figure 1e,f).

Q-factors up to 25800 for SWCNTs were measured, a value which exceeds by more than 2 orders of magnitude the values found in the literature[16,17] and by 3 orders of magnitude the fit inferred quality factor $Q_0 \simeq 20$ of the free SWCNT on the W tip in the absence of external stress. Measurements on graphene have also given important Q-factors of up to 5400, highly exceeding values found in literature.[3,14,18,27]

As mentioned above, an important pulling stress is induced in our samples by the electrostatic field that is controlled by the external voltage and it allows the storage of a high amount of vibration energy and, equivalently, guitar-like tuning of the resonance frequency over a wide range.[24] However, these dramatic increases in Q-factor highly exceed the "dilution of the dissipation" inherent with eigenfrequency up-tuning and are attributed here to the important decrease in the frequency width itself associated with viscoelastic damping (see eq 1). Moreover, this increase in Q-factor is enhanced by tunable "clamping softening", thus giving insight on the mechanism of gradual breaking of the clamping.

Four SWCNT samples (SWCNT1−4, Figure 1f) and one graphene sample (G1, Figure 1e) were tested by this method. First consider the SWCNTs. The voltage dependence of the harmonics $f_n(V_{DC})$ is now well understood[16,24,26,28] and is roughly a two parameter universal curve giving the increase in the eigenfrequency due to guitar-string-like mechanical stress and allowing determination of the eigenfrequency in the absence of stress from experimental data measured under stress, as detailed in and in the Supporting Information (SI). Figure 2a presents the experimental $f(V_{DC})$ dependence of the first two eigenmodes for SWCNT1, fitted as described below and in the Supporting Information. Note that although field emission can image even atomic scale objects, it does not allow measurements below a certain stress, given by the minimum V_{DC} that induces a detectable FE current. We can clearly observe in Figure 2a a very high stress regime where the measured eigenfrequency is increased with respect to the inferred zero voltage frequency by $\simeq \times 20$ for the first mode and $\simeq \times 10$ for the second mode. As the square of the angular eigenfrequency $\omega^2 = 4\pi^2 f^2$ of a harmonic oscillator is the restoring force per unit mass and per unit of displacement, in our system the restoring force due to electrostatic stress highly exceeds the intrinsic elastic restoring force. Although they have rather different eigenfrequencies, similar behavior is observed for SWCNT2 and SWCNT3, where the first mode's eigenfrequency is largely enhanced, $\simeq \times 100$, with respect to the fit inferred $V_{DC} = 0$ value. By comparison, SWCNT4 only exhibited $\simeq \times 3$ enhancement, as presented on Figure 2b.

This paper's main result is the dramatic increase in Q-factors of the SWCNTs with V_{DC}, presented in Figure 2c,d. For SWCNT1 (Figure 2c), the 1st mode's Q-factor increased by almost an order of magnitude from 3000 to more than 25 000 as V_{DC} was swept from 89 to 119 V, largely exceeding the 30% increase in eigenfrequency (see Figure 2a) and thus implying a strong decrease in the mode's width (see eq 1). The same behavior is observed on SWCNT2 and SWCNT3 where the strong increase of the Q-values are observed when electrostatic stress is applied via V_{DC} (Figure 2d). Similarly to its eigenfrequency, SWCNT4's Q-factor exhibited a smaller relative increase with V_{DC}, indicating a strong correlation between the mechanical axial stress and the dissipation of a mode. This correlation is equally observed on SWCNT1's 2nd mode, which has the same V_{DC} induced stress as the 1st mode, but more elastic stored energy due to more curvature and exhibits less relative increase in both eigenfrequency and Q-factor, as presented in Figure 2a,c. We can therefore reasonably

DOI: 10.1021/acs.nanolett.8b04282
Nano Lett. XXXX, XXX, XXX−XXX

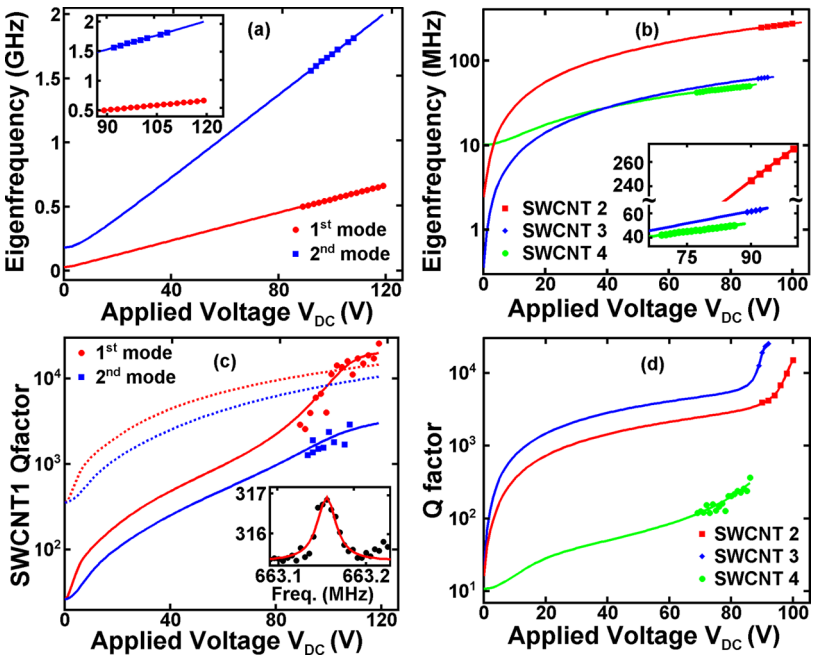

Figure 2. (a,b) Experimental (dots) and interpolated (solid line) eigenfrequency as a function of applied DC voltage curve for the first two eigenmodes of SWCNT1 (a) and for the first mode of SWCNT2−4 (b). The inset in (a) is a zoom on the experimentally available V_{DC} range. The frequency axis in (b) is logarithmic. The inset in (b) is a zoom on the experimental eigenfrequency points showing excellent quantitative agreement with fit. The frequency axis is linear and was discontinued for better readability. (c,d) Experimental (dots) and theoretical fits of the (solid line) quality factor as a function of applied DC voltage curve for the same samples as (a) for (c) and as (b) for (d). We observe a dramatic increase in Q-factor with V_{DC}, highly exceeding the eigenfrequency tuning presented on (a) and (b). The dotted lines in (c) show the Q-factor evolution fit if we consider only the viscoelastic contribution, which is clearly in much poorer agreement with experimental data than the solid line fit that also takes into account the clamping softening (see text and Supporting Information). The inset in (c) represents the experimental response for SWCNT1's 1st eigenmode (dots) for V_{DC} = 119 V with Lorentzian fit (solid line) giving Q = 25800. Note that solid lines fits in (a) and (c) were made at once for both the eigenfrequencies (a) and the Q-factors (c) and for the first two modes of SWCNT1 (dots and squares respectively). Similarly, solid lines fits in (b) and (d) were made at once for both the eigenfrequencies (b) and the Q-factors (d) for each one of SWCNT2, SWCNT3, and SWCNT4. For comparison with experiment, fitted complex eigenfrequencies were always represented in terms of real frequency and Q-factor.

conclude that energy loss is related to the flexural elastic stored energy and not to the stress energy as the SWCNTs vibrate.

Graphene samples grown by chemical vapor deposition[29,30] and transferred on W tips[31] (see also Supporting Information) also exhibited high Q-factors. As can be clearly observed in Figure 3a, graphene sample G1 was measured in a regime with lower guitar-string-like eigenfrequency tuning than the SWCNTs, due to less pronounced geometrical tip effects on the electrostatic field. We also observe a lesser influence of the mechanical motion on the emitted electrons, making low amplitude linear regime measurements very challenging. We present in Figure 3b a typical response curve with a slightly nonlinear behavior and fitted with a Duffing curve giving Q = 5400. Although measured in a moderate mechanical stress regime, this value is almost 2 orders of magnitude higher than typical room temperature Q-factors[14,18,27] and more than twice the highest value we found in literature.[3]

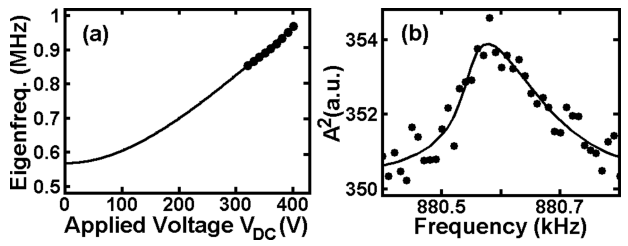

Figure 3. (a) Experimental (dots) and fit with the classical two parameter curve, as explained in the Supporting Information (solid line) eigenfrequency versus applied DC voltage curve for G1, indicating a moderate stress regime. (b) Experimental (dots) squared amplitude versus frequency response curve for V_{DC} = 340V, showing a slightly nonlinear regime. Fit (solid line) was made with the Duffing model and it gives a quality factor Q = 5400.

Viscoelastic dissipation, resulting from a delay between applied stress and resulting strain, is proportional to the flexural elastic stored energy for rod vibrations and therefore becomes the first choice candidate to explain the dramatic Q-factor increase with axial stress[32] (see also Supporting Information). Moreover, increasing axial stress, and its related stored energy, decreases the rod's curvature and localizes it to the clamped end,[33] diminishing the relative importance of the viscoelastic losses with respect to the total stored energy and giving therefore a more important increase in Q-factor than in the mode's eigenfrequency, that is, this effect surpasses a simple "dilution" of frequency width in increased resonance frequency, as inferred from eq 1.

Comparison of experimental data with theory uses the above-mentioned dependence of the eigenfrequencies on applied voltage in the absence of dissipation, as described in detail in ref 26 and in the Supporting Information. A first approach of introducing viscoelasticity with an imaginary part for the Young's modulus in the equations yields complex eigenfrequencies allowing to compute at the same time the V_{DC} dependence of the eigenfrequencies and of the Q-factors. The high-experimental precision on eigenfrequencies (Figure

DOI: 10.1021/acs.nanolett.8b04282
Nano Lett. XXXX, XXX, XXX−XXX

2a,b) imposes strict conditions for the less precisely measured Q-factors (Figure 2c,d). Although fits with energy losses exclusively due to viscoelasticity show important decrease in frequency width as V_{DC} is increased, they do not account for the whole dramatic increase in Q-factors, as presented on Figure 2c (dotted lines fit).

We attribute this difference in Q-factor enhancement to "soft clamping", somewhat similar to the behavior recently observed on phononic crystals with 10^6 bigger effective mass.[34] The effects of this "soft clamping" are increased by the localization of curvature and therefore of the flexural torque at the attached end of the SWCNT in the high stress regime.[33] Moreover, this high stress in our experiments, close to the clamping breaking limit, tunes the softening of the clamping itself. A simple phenomenological model of this behavior is a rotation oscillator, as presented on Figure 1b, where the spring constant decreases with the axial stress, vanishing at the breaking point (see Supporting Information). Resulting fits, when both viscoelasticity and tunable clamping softening are taken into account, give quantitative agreement of the measured $Q(V_{DC})$ dependence within experimental error and therefore explain the measured giant increase in Q-factor when stress is applied, as presented on Figure 2c,d (solid line fit). We have here not only a decrease in the frequency width Δf but a decrease in the dissipated energy E_D itself that allows the giant increase in the Q-factors. Note that the $Q(V_{DC} = 0)$ inferred values are roughly in the 10^1-10^2 range, slightly lower than values found in literature for room temperature measurements,[16,17] and are 2−3 orders of magnitude lower with respect to the maximum values on Figure 2c,d.

In summary we have shown that intrinsic material dissipation in graphene-based nanostructures is of viscoelastic nature and it can be dramatically reduced by applying external mechanical stress. This behavior, already seen on different materials with fixed prestress,[33] leads to extremely high Q-factors for SWCNTs and a graphene monolayer singly clamped on tips in our experiments and isolated as much as possible from the environment in order to suppress external dissipation channels. One way to understand why stress is so important for our samples is to notice that the elastic forces that generate mechanical resonances in the absence of applied voltages and induce viscoelastic losses scale with the size squared for same aspect ratio devices. For comparison, electrostatic forces inducing pulling are scale invariant for constant applied voltages, becoming overwhelming in our experiment for such small resonators in the high stress regime. Flexural vibration energy is stored in our system by three different mechanisms: flexural elastic spring deformation, deformation under stress like in a guitar string, and rotation at the clamping (see Supporting Information). Electrostatic-induced stress does not give rise to dissipation within experimental error in agreement with theoretical predictions for well conducting structures[6] while the flexural elastic spring energy is dissipated via viscoelasticity. Dissipation at clamping was neglected as it would give almost the same evolution of the Q-factor with stress for all modes, which is in contradiction with experimental results (see Supporting Information).

An interesting perspective of this work on single clamped SWCNT is extremely sensitive and atomically localized, force measurements at room temperature in an atomic force microscopy (AFM) configuration, for example, for few spin detection[36] or for quantum nature interaction measurements, like Casimir or van der Waals forces.[37] Although higher than cryogenic temperature values,[38] the inferred force noise $\sqrt{S_{FF}} < 1aN/\sqrt{Hz}$ for SWCNT1 and for SWCNT3 (see Supporting Information) is, to our knowledge, unprecedented for room-temperature experiments. Moreover, the Q/f coherence time for the graphene sample is around 6 ms, which is roughly 100 times superior to the coherence time for cryogenic quantum computer demonstrators.[39] As the Q-factor of mechanical resonators strongly increases when going to cryogenic temperatures,[14,15,19] such graphene samples could be interesting candidates for mechanical quantum bits if strongly enough coupled with nonlinear systems in order to create mechanical anharmonicity.[40]

■ ASSOCIATED CONTENT

Supporting Information

The Supporting Information is available free of charge on the ACS Publications website at DOI: 10.1021/acs.nanolett.8b04282.

Theoretical modeling and fit of experimental data, clamping breaking of the SWCNT samples, force noise estimation, SWCNT growth, graphene nanomanipulation, and excitation and detection of the resonances (PDF)

■ AUTHOR INFORMATION

Corresponding Author

*E-mail: sorin.perisanu@univ-lyon1.fr.

ORCID

S. Perisanu: 0000-0003-1408-2425

Notes

The authors declare no competing financial interest.

■ ACKNOWLEDGMENTS

The authors thank the R. Martel team from Université de Montréal for the graphene sample used in this study and C. Journet and N. Blanchard for helping us with the TEM images. This study was funded by the French National Research Agency (ANR) through the 3DX Online Project (ANR-15-CE08-0002-02).

■ REFERENCES

(1) Ekinci, K. L.; Roukes, M. L. *Rev. Sci. Instrum.* **2005**, *76*, 061101.
(2) Cagnoli, G.; Hough, J.; DeBra, D.; Fejer, M. M.; Gustafson, E.; Rowan, S.; Mitrofanov, V. *Phys. Lett. A* **2000**, *272*, 39−45.
(3) Barton, R. A.; Ilic, B.; Van der Zande, A. M.; Whitney, W. S.; McEuen, P. L.; Parpia, J. M.; Craighead, H. G. *Nano Lett.* **2011**, *11*, 1232−1236.
(4) Perisanu, S.; Vincent, P.; Ayari, A.; Choueib, M.; Bechelany, M.; Cornu, D.; Purcell, S. T. *Appl. Phys. Lett.* **2007**, *90*, 043113.
(5) Jourdan, G.; Torricelli, G.; Chevrier, J.; Comin, F. *Nanotechnology* **2007**, *18* (47), 475502.
(6) Barois, T.; Ayari, A.; Siria, A.; Perisanu, S.; Vincent, P.; Poncharal, P.; Purcell, S. T. *Phys. Rev. B: Condens. Matter Mater. Phys.* **2012**, *85* (7), 075407.
(7) Siria, A.; Barois, T.; Vilella, K.; Perisanu, S.; Ayari, A.; Guillot, D.; Purcell, S. T.; Poncharal, P. *Nano Lett.* **2012**, *12* (7), 3551−3556.
(8) Zhang, Y.; Moser, J.; Güttinger, J.; Bachtold, A.; Dykman, M. I. *Phys. Rev. Lett.* **2014**, *113* (25), 255502.
(9) Laird, E. A.; Pei, F.; Tang, W.; Steele, G. A.; Kouwenhoven, L. P. *Nano Lett.* **2012**, *12* (1), 193−197.
(10) Eichler, A.; Moser, J.; Chaste, J.; Zdrojek, M.; Wilson-Rae, I.; Bachtold, A. *Nat. Nanotechnol.* **2011**, *6*, 339−342.

DOI: 10.1021/acs.nanolett.8b04282
Nano Lett. XXXX, XXX, XXX−XXX

(11) Singh, V.; Bosman, S. J.; Schneider, B. H.; Blanter, Y. M.; Castellanos-Gomez, A.; Steele, G. A. *Nat. Nanotechnol.* **2014**, *9*, 820−824.
(12) Van Der Zande, A. M.; Barton, R. A.; Alden, J. S.; Ruiz-Vargas, C. S.; Whitney, W. S.; Pham, P. H. Q.; Park, J.; Parpia, J. M.; Craighead, H. G.; McEuen, P. L. *Nano Lett.* **2010**, *10* (12), 4869−4873.
(13) Moser, J.; Eichler, A.; Güttinger, J.; Dykman, M. I.; Bachtold, A. *Nat. Nanotechnol.* **2014**, *9*, 1007−1011.
(14) Chen, C.; Rosenblatt, S.; Bolotin, K. I.; Kalb, W.; Kim, P.; Kymissis, I.; Stormer, H. L.; Heinz, T. F.; Hone, J. *Nat. Nanotechnol.* **2009**, *4*, 861−867.
(15) Hüttel, A. K.; Meerwaldt, H. B.; Steele, G. A.; Poot, M.; Witkamp, B.; Kouwenhoven, L. P.; van der Zant, H. S. J. *Phys. Status Solidi B* **2010**, *247* (11), 2974.
(16) Sazonova, V.; Yaish, Y.; Üstünel, H.; Roundy, D.; Arias, T. A.; McEuen, P. L. *Nature* **2004**, *431*, 284−287.
(17) Gouttenoire, V.; Barois, T.; Perisanu, S.; Leclercq, J. L.; Purcell, S. T.; Vincent, P.; Ayari, A. *Small* **2010**, *6* (9), 1060.
(18) Garcia-Sanchez, D.; Van der Zande, A. M.; Paulo, A. S.; Lassagne, B.; McEuen, P. L.; Bachtold, A. *Nano Lett.* **2008**, *8* (5), 1399−1403.
(19) Jiang, H.; Yu, M. F.; Liu, B.; Huang, Y. *Phys. Rev. Lett.* **2004**, *93* (18), 185501.
(20) Jensen, K.; Kim, K.; Zettl, A. *Nat. Nanotechnol.* **2008**, *3*, 533−537.
(21) Pascale-Hamri, A.; Perisanu, S.; Derouet, A.; Journet, C.; Vincent, P.; Ayari, A.; Purcell, S. T. *Phys. Rev. Lett.* **2014**, *112* (12), 126805.
(22) Lassagne, B.; Tarakanov, Y.; Kinaret, J.; Garcia-Sanchez, D.; Bachtold, A. *Science* **2009**, *325* (5944), 1107−1111.
(23) Steele, G. A.; Httel, A. K.; Witkamp, B.; Poot, M.; Meerwaldt, H. B.; Kouwenhoven, L. P.; van der Zant, H. S. J. *Science* **2009**, *325* (5944), 1103−1107.
(24) Purcell, S. T.; Vincent, P.; Journet, C.; Binh, V. T. *Phys. Rev. Lett.* **2002**, *89* (27), 276103.
(25) Perisanu, S.; Vincent, P.; Ayari, A.; Choueib, M.; Bechelany, M.; Cornu, D.; Miele, P.; Purcell, S. T. *Phys. Status Solidi A* **2007**, *204* (6), 1645−1652.
(26) Perisanu, S.; Gouttenoire, V.; Vincent, P.; Ayari, A.; Choueib, M.; Bechelany, M.; Cornu, D.; Purcell, S. T. *Phys. Rev. B: Condens. Matter Mater. Phys.* **2008**, *77* (16), 165434.
(27) Bunch, J. S.; Van der Zande, A. M.; Verbridge, S. S.; Frank, I. W.; Tanenbaum, D. M.; Parpia, J. M.; Craighead, H. G.; McEuen, P. L. *Science* **2007**, *315* (5811), 490−493.
(28) Perisanu, S.; Barois, T.; Poncharal, P.; Gaillard, T.; Ayari, A.; Purcell, S. T.; Vincent, P. *Appl. Phys. Lett.* **2011**, *98*, 063110.
(29) Choubak, S.; Biron, M.; Levesque, P. L.; Desjardins, P.; Martel, R. *J. Phys. Chem. Lett.* **2013**, *4*, 1100.
(30) Choubak, S.; Levesque, P. L.; Gaufres, E.; Biron, M.; Martel, R.; Desjardins, P. *J. Phys. Chem. C* **2014**, *118*, 21532.
(31) Diehl, R.; Choueib, M.; Choubak, S.; Martel, R.; Perisanu, S.; Ayari, A.; Vincent, P.; Purcell, S. T.; Poncharal, P. Unpublished manuscript.
(32) Sandoval, F. A.; Geitner, M.; Bellon, L.; Bertin, E. *J. Appl. Phys.* **2015**, *117*, 234503.
(33) Unterreithmeier, Q. P.; Faust, T.; Kotthaus, J. P. *Phys. Rev. Lett.* **2010**, *105* (2), 027205.
(34) Ghadimi, A. H.; Fedorov, S. A.; Engelsen, N. J.; Bereyhi, M. J.; Schilling, R.; Wilson, D. J.; Kippenberg, T. J. *Science* **2018**, *360* (6390), 764−768.
(35) Marchand, M.; Journet, C.; Guillot, D.; Benoit, J.-M.; Yakobson, B.; Purcell, S. T. *Nano Lett.* **2009**, *9* (8), 2961−2966.
(36) Rugar, D.; Budakian, R.; Mamin, H. J.; Chui, B. W. *Nature* **2004**, *430*, 329.
(37) Mercier de Lépinay, L.; Pigeau, B.; Besga, B.; Vincent, P.; Poncharal, P.; Arcizet, O. *Nat. Nanotechnol.* **2016**, *12*, 156.
(38) Moser, J.; Güttinger, J.; Eichler, A.; Esplandiu, M. J.; Liu, D. E.; Dykman, M. I.; Bachtold, A. *Nat. Nanotechnol.* **2013**, *8*, 493−496.
(39) www.research.ibm.com/ibm-q/technology/devices/ (accessed on Feb 8, 2019).
(40) Tacchino, F.; Chiesa, A.; LaHaye, M. D.; Carretta, S.; Gerace, D. *Phys. Rev. B: Condens. Matter Mater. Phys.* **2018**, *97*, 214302.

DOI: 10.1021/acs.nanolett.8b04282
Nano Lett. XXXX, XXX, XXX−XXX